Environmental Effects on Cumulative Damage in Rocket Motors

R.A. Heller,* M.P. Singh,† and H. Zibdeh‡
Virginia Polytechnic Institute and State University, Blacksburg, Virginia

Cumulative damage in solid propellant rocket motors is induced by transient thermal stresses which, in turn, depend on ambient temperature, wind, and solar radiation, all functions of geographical location. It is shown that, contrary to the assumption that greatest damage occurs when stresses are large, the viscoelastic nature of the propellant can produce significant damage at lower stresses. As a consequence, protected storage is shown not alway to be beneficial to the service life of motors.

Nomenclature

$[A]$ = matrix of coefficients
a = absorptivity, $0 \le a \le 1$
a_T = damage parameter
C, C_1, C_2 = constants
$[D]$ = vector of known temperatures
D_n = cumulative damage
d_j = hourly damage
$E(t,T)$ = viscoelastic modulus, psi (N/m^2)
$E_\infty E_\ell$ = rest modulus, modulus of Maxwell elements
$F(t)$ = normal component of heat flux entering through cylinder surface, Btu/ft^2-h (W/m^2)
h = coefficient of surface heat transfer, Btu/h-ft^2-°F (W/m^2-C°)
h_c = heat convection coefficient, Btu/h-ft^2-°F (W/m^2-°C)
h_r = radiation heat transfer coefficient, Btu/h-ft^2-°F (W/m^2-°C)
I = incident radiation, Btu/ft^2-h (W/m^2)
i = index for motor layers, $i = 1,2,3,4,5$
j = index for time steps
K_i = thermal conductivity, Btu/ft-h-°F (W/m-°K)
Q = heat flux, Btu/ft^2-h (W/m^2)
Q_a = heat flux resulting from long-wave radiation emitted by the atmosphere
Q_c = heat transfer by convection
Q_g = heat flux by conduction into the cylinder
Q_i = heat flux resulting from incident short-wave radiation
Q_ℓ = heat flux resulting from long-wave radiation emitted by the cylinder surface
$Q_{\ell w}$ = reradiation
Q_n = absorbed short wave radiation
Q_r = heat flux resulting from reflected short-wave radiation
r_i = radius, in (m)
S_j = stress, psi (N/m^2)
$T(r,t)$ = space and time dependent temperature, °F (°C) or °R (°K)
T_0 = reference temperature, °R (°K)
T_{air} = ambient temperature, °F (°C)
T_{sky} = effective temperature of the sky, °F (°C)
V = average daily wind velocity, ft/s (m/s)
t_{fj} = time to failure at stress S_j, h
t = time (hours)
$[X]$ = vector of unknown temperatures
$\bar{\alpha}_i$ = thermal diffusivity, in^2/h (m^2/h)
$\bar{\alpha}_i$ = coefficient of thermal expansion in./in./°F (m/m/°C)
Δr_i = space increment
Δt = time increment
ΔT = temperature difference, °F (°C)
∂ = differential
ϵ = emissivity of the cylinder surface, $0 \le \epsilon \le 1$
ϵ_{as} = atmospheric emittance
ν_i = Poisson's ratio
σ = Stephan-Boltzmann constant, 0.1714×10^{-8} Btu/h-ft^2-°R^4 (5.688×10^{-8} W/m^2-°K^4)
τ_ℓ = relaxation time, h
ω_y = frequency of year
ω_d = frequency of day

Introduction

FIELD deployed rocket motors are stored in various geographical locations, with or without protective covering and under widely varying weather conditions. Depending on storage conditions, motors may be subjected to changing ambient temperatures, solar radiation, wind, rain, snow, etc. As a result, the propellant undergoes transient thermal stressing and concomitant cumulative damage.

Because shrinkage stresses are greatest at low storage temperatures, it has long been assumed that cumulative damage will follow a similar trend. The investigation presented here indicates, however, that such assumptions cannot be made for viscoelastic materials, where the shift function influences stresses and cumulative damage in varying degrees.

Hourly temperature, solar radiation, and wind speed records were obtained from the National Oceanic and Atmospheric Administration for two U.S. locations, one in the southwest and a second one in the Arctic. Motors were subjected to air temperature alone, simulating unconditioned storage-shed protection, to temperature combined with solar radiation and wind, respectively, (walls without roof and roof without walls), and finally to the combined effects of temperature, solar radiation, and wind (unprotected outdoor storage).

Presented as Paper 83-1120 at the AIAA/ASME/SAE 19th Joint Propulsion Conference, Seattle, Wash., June 27-29, 1983; received July 5, 1983, revision received Jan. 5, 1984.

*Professor, Department of Engineering Science and Mechanics. Associate Fellow AIAA.
†Professor, Department of Engineering Science and Mechanics.
‡Research Assistant, Department of Engineering Science and Mechanics.

For the purposes of transient temperature calculations, motors are assumed to be long cylinders with circular bores in either a bare condition or contained in an insulated canister as seen in Fig. 1. The conductive, convective, and radiative heat transfer problem was solved by an implicit finite difference scheme resulting in time series of temperatures at various locations in the propellant. Because temperature changes are relatively slow, thermal stresses are uncoupled, and stress analysis may be performed after temperatures at every point in the cylinder have been determined.

Though exact thermal stresses may be calculated,[1,2] a simplified stress analysis has been used in the present investigation because only relative effects of the various environmental influences were of interest.

Heat Exchange at the Cylinder Surface

Formulation

The rocket motor is considered to be a long axisymmetric cylinder (plane strain problem). The heat flow within the cylinder is modeled by the one-dimensional heat conduction equation

$$\frac{\partial^2 T(r,t)}{\partial r^2} + \frac{1}{r}\frac{\partial T(r,t)}{\partial r} = \frac{1}{\alpha}\frac{\partial T(r,t)}{\partial t} \tag{1}$$

Solar radiation and ambient temperature vary in intensitity around the circumference of the cylinder. However, it will be assumed in the present study that the cylinder receives uniform environmental input all around its circumference, because when the motor is inside an insulated container the propellant is relatively insensitive to short-term environmental variations. On the other hand, if the motor is bare, the high conductivity of the steel skin produces nearly uniform conditions.

From Fig. 1, the boundary conditions are as follows

B.C. 1 $$\left.\frac{\partial T}{\partial r}\right|_{r=r_1} = 0 \tag{2}$$

The bore is insulated

B.C. 2,4,6,8 $$(T_i(r_i,t) = T_{i+1}(r_i,t) \qquad i=1,2,3,4 \tag{3}$$

Temperatures at layer interfaces are continuous

B.C. 3,5,7,9 $$K_i\frac{\partial T_i(r_i,t)}{\partial r} = K_{i+1}\frac{\partial T_{i+1}(r_i,t)}{\partial r} \qquad i=1,2,3,4 \tag{4}$$

Heat fluxes are continuous through interfaces

B.C. 10 $$K_5\frac{\partial T(r_5,t)}{\partial r} + h(T-T_{\text{air}}) = aF(t) \tag{5}$$

The outer surface receives radiant, convective, and conductive input.

The last boundary condition makes it difficult to obtain a closed-form solution of this problem and, hence, a finite difference technique has been used.

Heat Balance Equation on the Surface of the Cylinder

Three forms of heat transfer take place on the cylinder surface, conduction, convection, and solar radiation.

Transfer of heat between the surface and the surrounding air is affected by wind speed, ambient temperature, solar radiation and type of the surface.

The energy balance equation on the surface is given as in Refs. 1 and 2:

$$Q_i - Q_r + Q_a - Q_\ell \pm Q_C \pm Q_g = 0 \tag{6}$$

Short-wave radiation is regarded as the part of the spectrum of solar radiation having wave lengths between 0.15 μ and 3.5 μ. It consists of two parts, direct and diffused radiation. Direct solar radiation is not reflected by clouds, absorbed, or scattered by the atmosphere. On the other hand, diffused solar radiation is reflected by clouds and absorbed or scattered by the atmosphere. The amount of both direct and diffused solar radiation reaching a horizontal surface is called global radiation. In the present study, several years of hourly observations of global radiation have been considered. These measurements were provided by the U.S. National Oceanic and Atmospheric Administration on magnetic tape.

Not all short-wave radiation will be absorbed by an object; some will be reflected. The amount of reflected radiation depends largely on the type and color of the surface.

In Eq. (6), Q_i and Q_r represent incident (both direct and diffused) and reflected short-wave radiation, respectively. In fact, one can combine these terms as

$$Q_n = Q_i - Q_r = aI_n \tag{7}$$

Long-wave radiation has wave lengths between 3.5μ and 150μ. This form of radiation is an exchange of heat energy between an object and the sky and arises from the fact that all bodies emit radiation.

The net long-wave radiation is the difference betwen that emitted from a unit area of the cylinder surface, denoted by Q_ℓ and reradiated by the atmosphere Q_a,

$$Q_{\ell w} = Q_\ell - Q_a = h_r(T - T_{\text{air}}) + \epsilon\sigma(T_{\text{air}}^4 - T_{\text{sky}}^4) \tag{8}$$

in which

$$h_r = \epsilon\sigma(T^2 + T_{\text{air}}^2)(T + T_{\text{air}}) \tag{9}$$

$Q_{\ell w}$ represents the so-called reradiation phenomenon which occurs continuously throughout the day and night. Since there is no short-wave radiation during the night, the reradiation renders the surface temperature lower than the ambient temperature.

Heat transfer by convection Q_c between the cylinder surface of temperature T and surrounding air is expressed as

$$Q_c = h_c(T_{\text{air}} - T) \tag{10}$$

The coefficient of heat convection, h_c, depends on wind velocity, the type of surface, and to a lesser extent, on temperature.

In the present study, an empirical relation proposed by Ulrich[3] will be used for the evaluation of h_c. This relation is

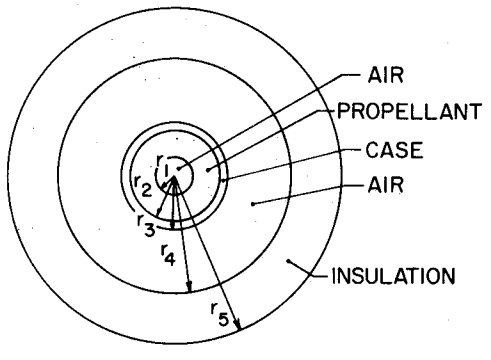

Fig. 1 Motor cross section.

applicable for a cylindrical object and is expressed in terms of its diameter D and the wind speed V

$$h_c = 0.6\left(\frac{V}{D}\right)^{0.5} \quad \text{if} \quad 6\times10^{-4} < VD < 6$$

or

$$h_c = 1.0\left(\frac{V}{D}\right)^{0.5} \quad \text{if} \quad 6 < VD < 60$$

With these relations, the boundary condition, Eq. (5), on the surface, can be expressed as

$$-K\frac{\partial T}{\partial r} = (h_c + h_r)(T - T_{\text{air}}) + \epsilon\sigma(T_{\text{air}}^4 - T_{\text{sky}}^4) - aI_n \qquad (11)$$

in which $h_c + h_r \simeq h$ and is referred to as the coefficient of surface heat transfer. The value of h_r is determined here by an iterative process whereby the surfce temperature is first assumed in Eq. (9) and is used to calculate an improved temperature from Eq. (11). The process is repeated until a stabilized h_r is obtained.

Finite Difference Solution[4]

Utilizing the Taylor expansion of a function $T(r)$ about a point i and neglecting terms higher than second order, the left side of Eq. (1) becomes

$$\frac{\partial^2 T}{\partial r^2} + \frac{1}{r}\frac{\partial T}{\partial r} = \frac{1}{\Delta r}\left\{\frac{1}{2r}T_{i+1} + \frac{1}{\Delta r}T_{i+1} - \frac{2}{\Delta r}T_i - \frac{1}{2r}T_{i-1} + \frac{1}{\Delta r}T_{i-1}\right\} \qquad (12)$$

A second-order correct expression for the time derivative at the point r_i and time $t_{j+\frac{1}{2}}$ is used[5]

$$\left(\frac{\partial T}{\partial t}\right)_{i,j+\frac{1}{2}} = \frac{T_{i,j+1} - T_{i,j}}{\Delta t} - \left(\frac{\partial^3 T}{\partial t^3}\right)_{i,j+\frac{1}{2}}\frac{(\Delta t)^2}{24} - \cdots \qquad (13)$$

With the Crank-Nicholson[5] and the Galerkin scheme of averaging, a factor $\theta = 2/3$ and Eq. (13) are introduced into Eq. (12):

$$\frac{1}{\alpha}\frac{T_{i,j+1} - T_{i,j}}{\Delta t} = \frac{\theta}{\Delta r}\left\{\left(\frac{1}{\Delta r} - \frac{1}{2r}\right)T_{i-1,j+1} - \frac{2}{\Delta r}T_{i,j+1} + \left(\frac{1}{\Delta r} + \frac{1}{2r}\right)T_{i+1,j+1}\right\} + \frac{(1-\theta)}{\Delta r}\left\{\left(\frac{1}{\Delta r} - \frac{1}{2r}\right)T_{i-1,j} - \frac{2}{\Delta r}T_{i,j} + \left(\frac{1}{\Delta r} + \frac{1}{\Delta r}\right)T_{i+1,j}\right\} \qquad (14)$$

where the error is of the order of $0(\Delta r^2)$ and $0(\Delta t^2)$.

Boundary condition 1, at the bore of the cylinder may be developed[1] in finite difference form as

$$\frac{1}{\alpha}\frac{T_{1,j+1}}{\Delta t} - \frac{4\theta}{\Delta r^2}(T_{2,j+1} - T_{1,j+1}) = \frac{1}{\alpha\Delta t}T_{1,j} + \frac{4(1-\theta)}{\Delta r^2}(T_{2,j} - T_{1,j}) \qquad (15)$$

Boundary conditions 3, 5, 7, and 9 along the interfaces, expressed in finite difference form, become

$$-\frac{K_i}{2\Delta r_i}T_{m-2,j+1} + \frac{2K_i}{\Delta r_i}T_{m-1,j+1} - \left(\frac{3K_i}{2\Delta r_i} + \frac{3K_{i+1}}{2\Delta r_{i+1}}\right)T_{m,j+1} + \frac{2K_{i+1}}{\Delta r_{i+1}}T_{m+1,j+1} - \frac{K_{i+1}}{2\Delta r_{i+1}}T_{m+2,j+1} = 0 \qquad (16)$$

where m is the point on the boundary. Finally, the boundary condition on the surface, is written with the introduction of a shape factor s for the cylindrical surface as

$$-\frac{2\theta}{\Delta r^2}T_{i-1,j+1} + \left[\frac{1}{\alpha\Delta t} + \frac{2\theta}{\Delta r^2} + \frac{h}{K}\theta\left(\frac{1}{r} + \frac{2}{\Delta r}\right)\right]T_{i,j+1}$$

$$= \frac{2}{\Delta r^2}(1-\theta)T_{i-1,j} + \left[\frac{1}{\alpha\Delta t} - \frac{2(1-\theta)}{\Delta r^2} - \left(\frac{1}{r} + \frac{2}{\Delta r}\right)(1-\theta)\frac{h}{K}\right] \times T_{i,j} + \left(\frac{1}{r} + \frac{2}{\Delta r}\right)(1-\theta)\frac{h}{K}T_{\text{air},j} + \left(\frac{1}{r} + \frac{2}{\Delta r}\right)\frac{h}{K}\theta T_{\text{air},j+1}$$

$$+ \frac{\theta}{K}\left(\frac{1}{r} + \frac{2}{\Delta r}\right)[as\ I_{n,j+1} - \epsilon\sigma(T_{\text{air},j+1}^4 - T_{\text{sky}}^4)] + \frac{(1-\theta)}{K}\left(\frac{1}{r} + \frac{2}{\Delta r}\right) + \frac{(1-\theta)}{K}\left(\frac{1}{r} + \frac{2}{\Delta r}\right) \times (as\ I_{n,j} - \epsilon\sigma(T_{\text{air},j}^4 - T_{\text{sky}}^4)] \qquad (17)$$

T_{sky} was proposed and used by Ulrich[6] as

$$T_{\text{sky}} = T_{\text{air}} - 20 \qquad (18)$$

where T_{sky} and T_{air} are absolute temperatures.

Equations (14-16) provide a set of simultaneous algebraic equations, solved here by the Gaussian elimination method.

In matrix form, these equations are written as

$$[A][X] = [D] \qquad (19)$$

where $[A]$ represents the matrix of coefficients, $[X]$ is a column vector representing the unknown temperature at a time of interest, say t_{j+1}, and the column vector $[D]$ includes the tempertures (known) at the present time, t_j.

For a given initial temperature across the cylinder with n nodes, one can obtain the temperature of these nodes at the next time step. Next, these new temperatures are used as known variables in Eq. (18) to obtain temperatures of n nodes at yet another time step.

Cumulative Damage

For a given temperature distribution across the web of the motor, stresses may be calculated utilizing viscoelastic stress-strain relations and equations developed in Refs. 7-9. Because the object of the present study is to compare the relative cumulative damages (induced by various environmental inputs), lengthy and expensive motor-stress calculations are not carried out. A simple stress equation that utilizes the momentary value of the viscoelastic modulus, $E(t,T)$ and the calculated bore temperature will instead by used:

$$S = -10\times E(t,T)\,\bar{\alpha}\Delta T \qquad (20)$$

The factor 10 is applied so that stresses of the order of magnitude of the bore tangential stress should result.

An examination of Table 1 indicates that actual motor stresses are of the same order of magnitude as those given by Eq. (20).

The value of the viscoelastic modulus is calculated from a master curve expanded into a Prony series as

$$E(t,T) = E_\infty + E'(t,T) \tag{21}$$

where

$$E'(t,T) = \sum_{\ell=1}^{n} E_\ell e^{-t/\tau_\ell a_T} \tag{22}$$

and $E'(t,T) \to 0$ as $t \to \infty$ and the shift function a_T follows the Williams, Landell, Ferry (W.L.F.) equation

$$\log a_T = \frac{-C_1(T-T_0)}{C_2+(T-T_0)} \tag{23}$$

The linear cumulative damage rule proposed by Palmgren[10] and Miner[11] has been used extensively in the aerospace industry. According to this rule, the damage produced in a unit of time spent at a particular stress level S_j is inversely proportional to the time t_{fj} required to produce failure in the material at that stress level

$$d_j = 1/t_{fj} \tag{24}$$

When a mixture of n stress levels is present each for a time Δt the total damage D becomes equal to

$$D_n = \sum_{j=1}^{n} \frac{\Delta t}{t_{fj}} \tag{25}$$

Experiments conducted by Bills[12] indicate that the linear cumulative damage rule may be useful in the prediction of service life of solid propellants. It has also been shown that a power function will describe the relationship between applied constant stress and reduced time to failure

$$t_{fj}/a_{Tj} = CS_j^{-B} \tag{26}$$

where material parameters C and B are listed in Table 2 and S is the stress of Eq. (20). Hence cumulative damage after n

Table 1 Actual and approximate maximum and minimum motor stresses

	Motor stresses, psi			
	Maximum for year		Minimum for year	
	Actual	Eq. (20)	Actual	Eq. (20)
Phoenix, Arizona	16.20	18.73	10.90	12.10
Alaskan Arctic	32.68	36.4	21.56	24.1

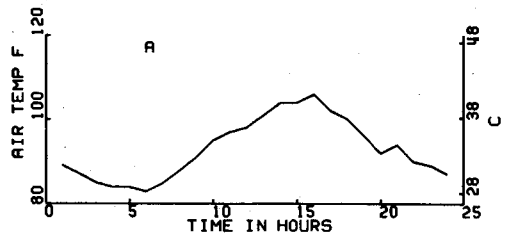

Fig. 2a Phoenix, Arizona summer day air temperature.

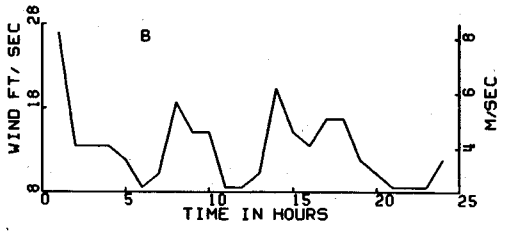

Fig. 2b Phoenix, Arizona summer day wind speed.

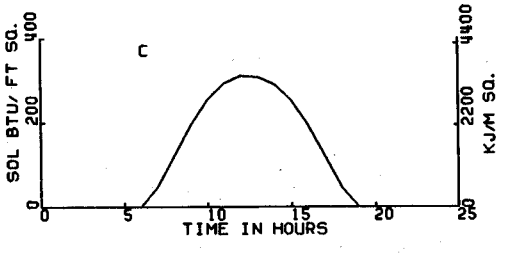

Fig. 2c Phoenix, Arizona summer day solar radiation.

Table 2 Parameters of motor material

Parameter	Air	Propellant	Steel
Radius, m (in.)	0.048 (1.875)	0.109 (4.300)	0.112 (4.400)
Thermal conductivity, W/m – °C (Btu/h-ft – °F)	0.025 (0.015)	1.322 (0.764)	25.25 (14.600)
Diffusivity, m^2/s (ft^2/h)	0.197×10^{-4} (0.760)	0.785×10^{-6} (0.030)	0.877×10^{-5} (0.340)
Coefficient of thermal exp. m/m/°C (in./in./°F)		1.04×10^{-4} (5.78×10^{-5})	1.17×10^{-5} (6.50×10^{-6})
Poisson's ratio, ν		0.49	0.25
Modulus E_∞, N/m^2 (psi)		1.943×10^6 (281.840)	2.068×10^{11} (30×10^6)
Viscous modulus, E_1 N/m^2 (psi)		0.150×10^7 (0.204×10^3)	
Viscous modulus, E_2 N/m^2 (psi)		0.188×10^7 (0.272×10^3)	
Relaxation times, h			
τ_1		9.25×10^{-6}	
τ_2		9.25×10^{-4}	
Shift function, T in °F			
$\log a_T = 1.42\left[\frac{-8.86(T+34.6)}{182+(T+34.6)} + 3.32\right]$			
Cumulative damage, stress, N/m^2 time, h			
C		5.491×10^{49}	
B		8.75	
Stress free temperature, °C (°F)		74 (165)	

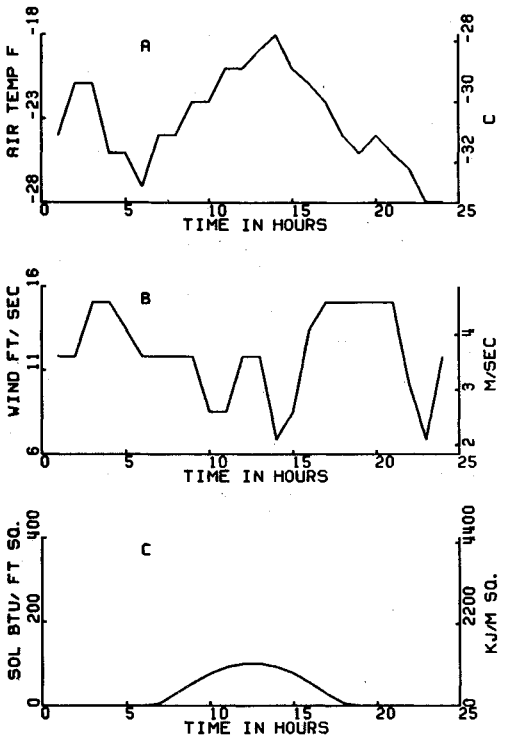

Fig. 3 Alaska winter day: a) air temperature, b) wind speed, c) solar radiation.

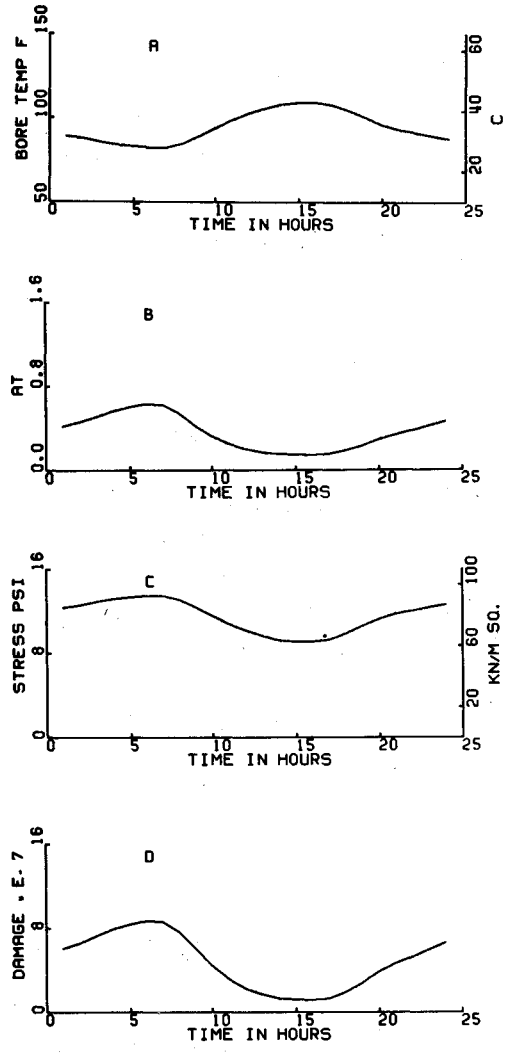

Fig. 4 Phoenix, Arizona summer day (Fig. 2): a) bore temperature, b) shift function, c) pseudostress, d) damage.

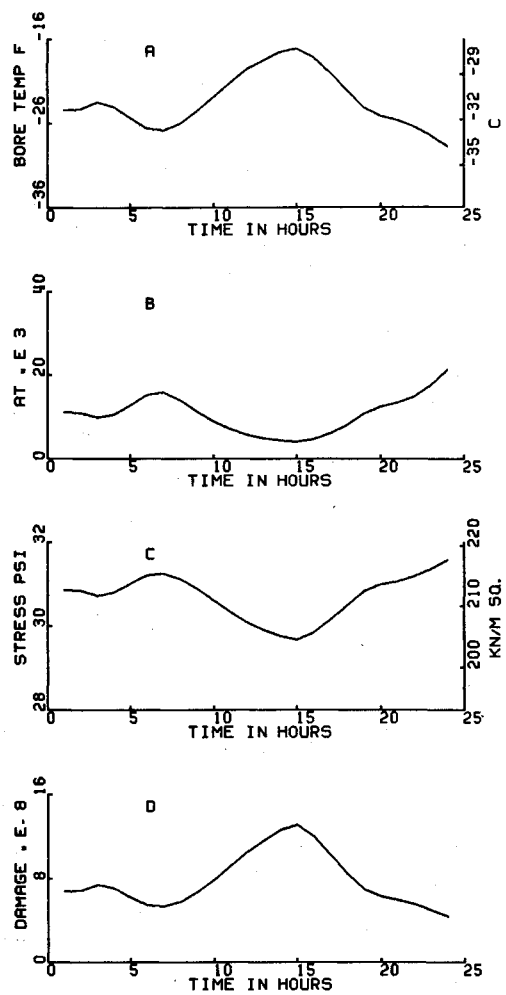

Fig. 5 Alaska winter day (Fig. 3): a) bore temperature, b) shift function, c) pseudostress, d) damage.

time steps may be expressed as

$$D_n = \frac{1}{C} \sum_{j=1}^{n} \frac{\Delta t S_j^B}{a_{Tj}} \tag{27}$$

The shift function appears explicitly in the denominator of Eq. (27) and also implicitly through the modulus and stress.

Cumulative Damage Under Environmental Conditions

In order to examine the relative amounts of damage produced at storage sites with extreme conditions, two locations were chosen. A three-month period during the summer in Phoenix, Arizona, and a winter period of a similar length in the Alaskan Arctic were used, first to calculate damage in an uninsulated motor with ambient temperature, wind, and solar radiation included, that is under unprotected outdoor storage conditions. Subsequently, temperature alone (storage shed), temperature and wind (roof but no walls), and finally, temperature and radiation (walls without roof) were applied to the motor and relative damages were compared.

Hourly observations of the National Oceanic and Atmospheric Administration at the two sites were fed into the finite difference equations and tempertature-time histories were calculated for a motor whose geometry and thermal parameters are listed in Table 2.

The ambient temperature, wind speed and solar radiation in Phoenix on a summer day are presented in Fig. 2 for a typical 24-h period. A similar set of graphs are plotted in Fig. 3 for a late winter day in Alaska. The resulting bore temperatures, shift functions, pseudostresses, and damages are shown in Figs. 4 and 5.

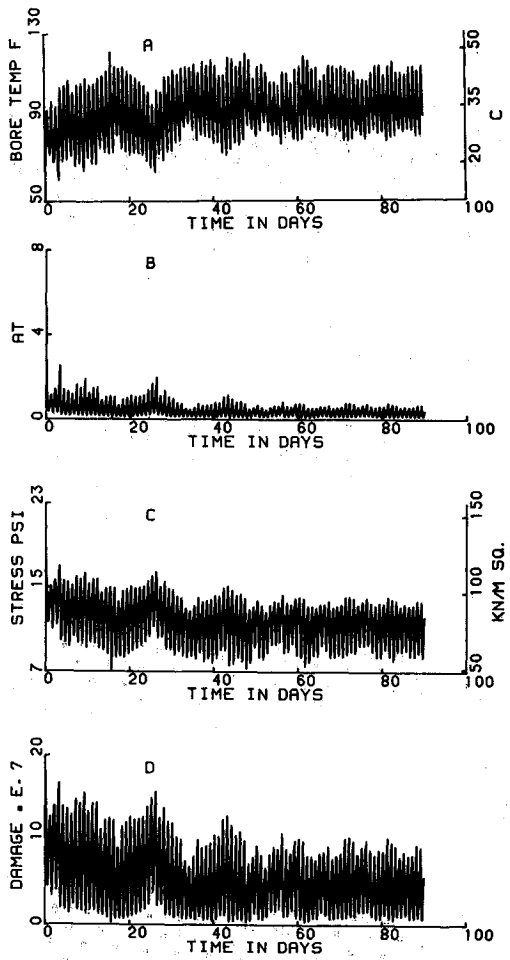

Fig. 6 90-day summer period in Phoenix, Arizona: a) bore temperature, b) shift function, c) pseudostress, d) damage.

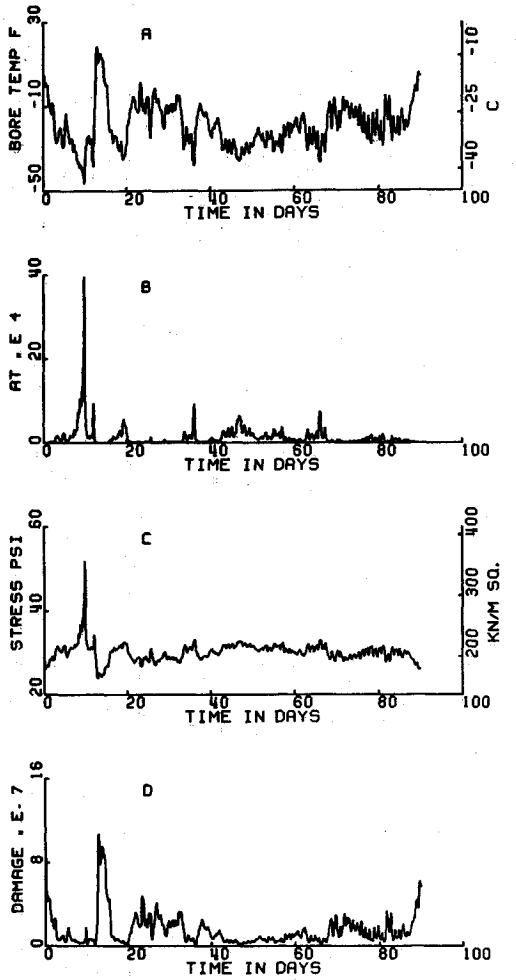

Fig. 7 90-day winter period in Alaska: a) bore temperature, b) shift function, c) pseudostress, d) damage.

Table 3 90-day accumulated damage

Fig. 8	1952	0.00184
	1954	0.00195
	1962	0.00182
Fig. 9	1952	0.00018
	1954	0.00042
	1962	0.00050
Fig. 10a		0.00184
Fig. 10b		0.00142
Fig. 10c		0.00120
Fig. 10d		0.00106
Fig. 11a		0.00018
Fig. 11b		0.00031
Fig. 11c		0.00032
Fig. 11d		0.00021

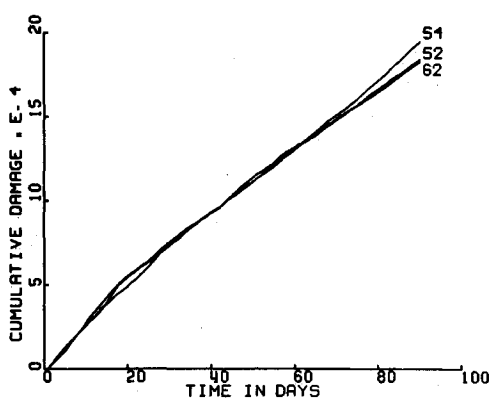

Fig. 8 90-day summer cumulative damage in 1952, 1954, and 1962 in Pheonix, Arizona.

Differences in the damage produced are unexpected. Though stresses are considerbly lower during a summer day in Phoenix than on a winter day in Alaska, damage is greater in Arizona. It is evident from an examination of the figures and Eq. (27) that the shift parameter, a_T, affects damage formation inversely. Hence, when its value is small, as is the case in Arizona, damage is large, while the converse is true in Alaska.

The same effects are seen in Figs. 6 and 7 over a 90-day period at the two sites. In a cold environment, even small temperature changes result in large variations in the shift function, while changes in stresses are relatively minor. Consequently an increase in damage is observed (Fig. 7d) whenever a_T drops to lower values. The warm temperatures in Arizona, on the other hand, produce only small changes in a_T as well as in stress, and consequently damage changes are more gradual (Fig. 6d). Again, damage is greater in Phoenix than in Alaska.

It is also interesting to observe that in Phoenix damage follows a daily cycle, while in Alaska this variation is missing. It should be remembered that there is no actual day or night in the Arctic because the Sun stays below the horizon during the six months of winter. The year-to-year variations of cumulative damage have also been examined for three in-

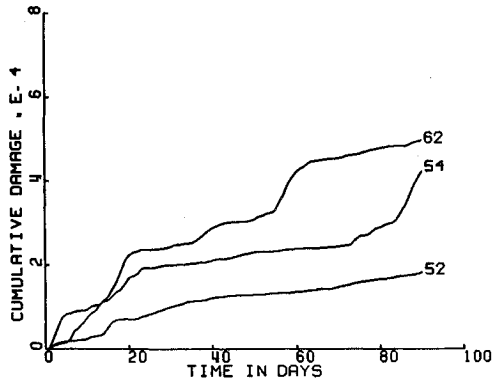

Fig. 9 90-day winter cumulative damage in 1952, 1954, and 1962 in Alaska.

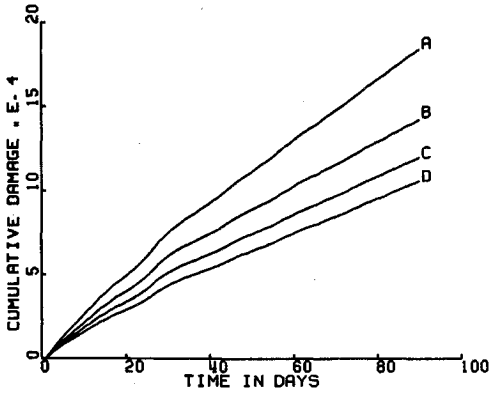

Fig. 10 90-day cumulative damage (summer, Arizona); line A = temperature alone, line B = temperature and wind, line C = temperature, wind, and radiation, line D = temperature and radiation.

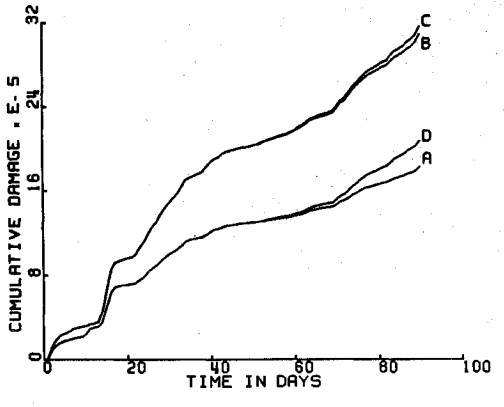

Fig. 11 90-day cumulative damage (winter, Alaska); line A = temperature alone, line B = temperature and wind, line C = temperature, wind, and radiation, line D = temperature and radiation.

dividual years with severe winters at the two sites. Figures 8 and 9 present the results for the years 1952, 1954, and 1962 at Phoenix and in Alaska.

While in summer the variations are quite small, the Arctic winter does affect damage differently each year. It is, however, not possible to determine the severity of a particular year without a complete thermal analysis. The lowest temperature in 25 years was recorded as $-54°F$ ($-48°C$) in 1954, but damage was less in that year than in 1962.

Storage Conditions and Cumulative Damage

The damaging effects of various storage conditions are indicated in the next set of figures. Temperature effects alone (indoor but unheated storage) were compared with combined temperature, wind, and radiation-induced damage (unprotected outdoor storage) and with temperature-wind and temperature-radiation (roof but no walls and walls but no roof, respectively) results. Cumulative damage over a 90-day period during a typical suymmer is presented in Fig. 10 for Phoenix. Here, indoor storage proves to be more damaging then unprotected outdoor deployment, while in the Alaskan winter (Fig. 11) the situation is reversed. At both locations, wind has alleviating effects. The individual damages are presented in Table 3.

These obserations are all traceable to variations in the shift function relative to those in stress. It is, however, not feasible to determine the most favorable storage conditions by examining temperature histories alone, and a complete thermal-stress analysis must be performed for each type of motor.

Conclusions

Contrary to intuition, a cumulative damage analysis under environmental thermal stressing of solid propellants indicates that for some materials, greater damage is produced by high temperatures than by low ones. Damage is significantly affected by the time-temperature shift function and to a lesser extent by thermal stress. An investigtion of various storage methods indicates that an optimum protective arrangement may be derived for each geographic location and that in certain instances an unprotected motor will experience less damage than a protected one.

References

[1] Con, V.N., "Finite Difference Approach for Predicting Probabilistic Life of a Composite Cylinder Subjected to Thermal Random Loads," Ph.D. Dissertation, Dept. of Engineering Mechanics, Virginia Polytehnic Institute, Blacksburg, Va., March 1979.

[2] Con, V.N., Heller, R.A., Singh, M.P., and Tuyen, L.D., "Thermal Stress in a Composite Cylinder by Finite Difference Technique," Paper No. 80-HT-107, *ASME/AICHE Heat Transfer Meeting*, Orlando, Fla., July 27-30, 1980.

[3] Ulrich, R.D., "Evolution of the NWC Thermal Standard," NWC TP 4834, Part 1, Naval Weapons Center, China Lake, Calif., Feb. 1970.

[4] Rosenburg, D.U., *Method for the Numerical Solution of Partial Differential Equations*, American Elsevier Publishing Co., Inc., New York, 1969, p. 23.

[5] Cranck, J. and Nicolson, P., "A Practical Method for Numerical Evaluation of Solution of Partial Differential Equation of the Heat Conduction Type," Proceedings of the Cambridge Philosophical Society, Vol. 43, 1947, pp. 50-67.

[6] Ulrich, R.D., "Evolution of the NWC Thermal Standard," NWC TP 4834,Part 3, Naval Weapons Center, China Lake, Calif., May 1977.

[7] Heller, R.A., Kamat, M.P., and Singh, M.P., "Probability of Solid Propellant Motor Failure Due to Environmental Temperatures," *Journal of Spacecraft and Rockets*, Vol. 6, May-June 1979, pp. 140-146.

[8] Williams, M.L., Blatz, P.J., and Shapery, R.A., "Fundamental Studies Relating to Systems Analysis of Solid Propellants," GALCIT, SM 61-5, California Institute of Technology, Pasadena, Calif., 1961, pp. 165-166.

[9] Heller, R.A. and Singh, M.P., "Thermal Storage Life of Solid Propellant Motors," *Journal of Spacecraft and Rockets*, Vol. 20, April 1983, pp. 144-149.

[10] Palmgren, A., "Die Lebensdauer von Kugellagern," Verein Deutscher Ingenieure Zeitschrift, Vol. 68, No. 14, 1924, p. 339.

[11] Miner, M.A., "Cumulative Damage in Fatigue," *Journal of Applied Mechanics*, Vol. 12, 1945, p. A-159.

[12] Bills, K.W., Jr. and Wiegand, J.H., "The Application of an Integrated Structrual Analysis to the Prediction of Reliability," *Annals of Reliability and Maintainability*, 1970, pp. 514, 526.